frontiers | Frontiers in Quantum Science and Technology

TYPE Original Research
PUBLISHED 29 December 2025
DOI 10.3389/frqst.2025.1725290



OPEN ACCESS

EDITED BY
Sebastiano Pilati,
University of Camerino, Italy

REVIEWED BY
Xianlong Gao,
Zhejiang Normal University, China
Guilherme Almeida,
Federal University of Alagoas, Brazil

*CORRESPONDENCE
Iara Patrícia Da Silva Ramos,
iara.ramos@ufrgs.br
Rafael Gandolfi Lanzini,
rafael.lanzini@ufrgs.br
Leonardo Brunnet,
leon@if.ufrgs.br
Sandra D. Prado,
prado@if.ufrgs.br

RECEIVED 16 October 2025
REVISED 08 December 2025
ACCEPTED 11 December 2025
PUBLISHED 29 December 2025

CITATION
Da Silva Ramos IP, Gandolfi Lanzini R, Brunnet L and Prado SD (2025) Correlated disorder as a tunable switch between trapping and conduction in quantum ion channels. *Front. Quantum Sci. Technol.* 4:1725290. doi: 10.3389/frqst.2025.1725290



# Correlated disorder as a tunable switch between trapping and conduction in quantum ion channels

Iara Patrícia Da Silva Ramos*, Rafael Gandolfi Lanzini*, Leonardo Brunnet* and Sandra D. Prado*

Institute of Physics, Federal University of Rio Grande do Sul, Porto Alegre, Rio Grande do Sul, Brazil

Quantum transport efficiency is influenced by mechanisms beyond coherence, including correlated disorder, which can balance localization and mobility to produce anomalous phenomena such as quantum rogue waves. Motivated by recent findings, we investigate the impact of correlated on-site energies in a linear quantum chain modeling a biological ion channel. The system is described by a tight-binding Hamiltonian with Lindblad operators representing source and drain. The average traversal time across the channel increases logarithmically with the correlation parameter, mirroring the growth of rogue-wave probability and indicating the emergence of temporary trapped states that slow transport. These results demonstrate that correlated disorder significantly influences ion transport even in small disordered systems.

KEYWORDS

**conduction, correlated disorder, quantum ion channels, tight-binding Hamiltonian, trapping localization**

## 1 Introduction

All living organisms share a fundamental characteristic: the presence of cells. Traditionally regarded as the basic structural and functional units of life, cells have also been described, according to Salari et al. (2017), as nano-machines capable of replication and information processing. This perspective not only emphasizes their complexity but also aligns with growing evidence of quantum mechanical phenomena in biological systems. For example, quantum coherence has been demonstrated in photosynthetic complexes during exciton energy transfer (Engel et al., 2007; Mohseni et al., 2008; Collini et al., 2010).

In addition, quantum superposition has been reported at the single-electron and single-photon levels in chiral molecular systems (Aiello et al., 2022), while quantum entanglement has been proposed as a mechanism underlying avian magnetoreception and navigation (Hore and Mouritsen, 2016). Specifically, the coherent spin dynamics of radical pair reactions, hypothesized to underlie avian magnetoreception, present a prime area for the application of digital quantum simulation (DQS) techniques on near-term hardware (Alvarez et al., 2024) or even in light-harvesting components of photosynthetic organisms (Sarovar et al., 2010).

Furthermore, quantum tunneling has been suggested to contribute to processes such as genetic mutations (McFadden and Al-Khalili, 1999), olfactory perception, and enzymatic catalysis (Brookes, 2017). These examples illustrate how quantum mechanical principles may underlie a wide range of biological processes, particularly those involving transport

10.3389/frqst.2025.1725290

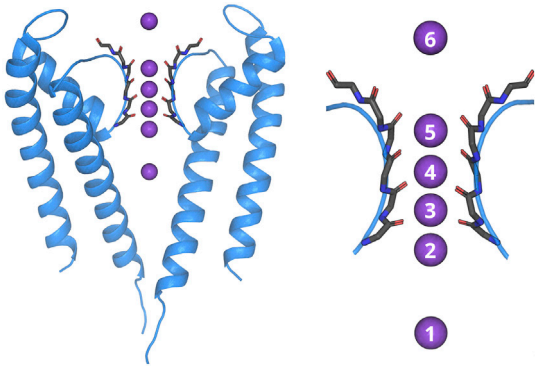


FIGURE 1
Structure of the selectivity filter (SF), which comprises four potassium-binding sites formed by carbonyl groups and oxygen atoms (in red), as well as an external $K^+$ binding site (Doyle et al., 1998) (site 6 in our equations). In our model, site 1 is defined as the source, sites 2 to 5 constitute the ion channel, and site 6 acts as the drain.

mechanisms. Since transport processes are essential for the functioning of biological systems, ion channels represent a critical case.

Ion channels are membrane-embedded proteins that play a crucial role in the propagation of electrical signals across cell membranes. They mediate the selective passage of ions through specialized pore structures. A defining feature of these channels is their remarkable ion selectivity, which is largely determined by a structural region known as the selectivity filter (SF), as illustrated in Figure 1.

Structural studies, particularly X-ray crystallography of the KcsA channel from the bacterium Streptomyces lividans, have provided detailed information about the SF, revealing an approximate diameter of 0.3 nm and a length of 1.2 nm (Doyle et al., 1998). The thermal energy of the potassium ion can be calculated as approximately $2 \times 10^{-7}$ J, with a corresponding de-Broglie wavelength matter wave of approx. 0.05 nm (Vaziri and Plenio, 2010).

Since the thermal wavelength and dimensions of the SF are within a compatible order of magnitude, it is possible to view the transport of ions as a diffraction of the potassium wave matter off a one-dimensional series of potential wells formed by the SF binding sites. Despite these important insights, the precise molecular mechanisms underlying ion selectivity remain incompletely understood and continue to be actively investigated by the scientific community. In line with the tetrameric structure of the SF discussed by Doyle et al. (1998), which has four coordination sites, our model uses a linear chain of 6 sites (4 channel sites plus source and drain) as shown in Figure 1.

According to Vaziri and Plenio, (2010), quantum coherence may play a role in the selectivity and ion conduction of the SF. The authors propose that the mechanisms underlying high conduction rates and ion discrimination, as observed in potassium channels such as KcsA, may have a quantum origin, involving diffraction of the potassium matter wave or quantum tunneling through potential barriers. Their work also suggests an alternative experimental approach to ultrafast two-dimensional spectroscopy by showing that the application of an external alternating electric field (AC) could induce resonances in ion channel conductivity signatures of quantum coherence in the system.

Quantum coherence is a key factor underlying the high efficiency of quantum transport (Polakowski and Panfil, 2024). However, in realistic systems, interactions with the environment or with phonons arising from protein structural fluctuations introduce inevitable noise and disorder (Plenio and Huelga, 2008; Jalalinejad et al., 2018; Almeida et al., 2018). These fluctuations can disrupt coherence and modify transport properties. Depending on their nature, the resulting disorder may be completely random or exhibit spatial correlations (Izrailev et al., 2012). Understanding how such correlated disorder influences transport is therefore essential, particularly in open quantum systems that model biological ion channels, where coupling to external reservoirs and internal structural dynamics play a fundamental role.

A recent study by Buarque et al. (2023) shows that spatially correlated site energies in a one-dimensional lattice with hopping can produce highly localized intensities in the wave functions due to anomalous quantum amplitudes, controlled by a parameter that sets the correlation length. Similar effects have also been observed in a variety of wave phenomena, from ocean waves to optical systems (da Silva and Prado, 2020; Bonatto et al., 2020). Nonetheless, the role of correlated disorder in transport efficiency within open quantum systems that simulate the selectivity filter (SF) of ion channels, modeled as small lattices with a source and a drain, has not yet been fully explored. The selectivity filter is an open system in contact with ionic reservoirs and is characterized by structural fluctuations which might introduce disorder into the site energies.

In this work, we address this gap by investigating transport dynamics in an open quantum system inspired by the KcsA selectivity filter structure under the influence of correlated disorder. We employ the Lindblad master equation to model the SF coupled to a source and a drain. The disorder is introduced into the on-site potentials using a method that allows explicit control over the correlation length. Although a six-site lattice would not ordinarily be expected to capture the subtleties introduced by spatial correlations, our ensemble analysis with 10,000 disorder realizations shows that the mean traversal time increases significantly under strong on-site potential correlations. This demonstrates that the underlying mechanism responsible for correlation-induced delays persists even in small open systems, a result that is both unexpected and noteworthy, and which we aim to highlight in this paper.

The remainder of this paper is organized as follows. Section 2 introduces the theoretical model used to simulate ion transport through the channel and outlines the governing dynamical equations. Section 3 presents the numerical results and discusses their physical implications in the context of correlated disorder and environmental effects. Section 4 summarizes the main conclusions and relates our findings to the mechanisms of ion transport in ion-channel systems.

## 2 Model and methods

We modeled the selectivity filter (SF) as a linear lattice composed of a source (site 1), four sites (2–5) representing the ion channel and a drain (site 6) (see Figure 1). The source acts as an emitter to the

channel, while the extracellular site (site 6) acts like a drain, removing particles from the channel. The entry and exit processes are irreversible: once a particle enters the channel, it cannot return to the source. This configuration was adopted to simulate the interaction between the SF and its surrounding environment.

According to experimental studies (Berneche and Roux, 2001; Gwan and Baumgaertner, 2007), the distance between two adjacent potential minima is approximately 0.24 nm, requiring each ion to cross an energy barrier Δ. It has been found that the average height of this barrier fluctuates between 1.7 and 8.0 $k_BT$, while its width Δ is smaller than the distance between successive sites. Ion transmission across the barrier therefore involves quantum tunneling between neighboring binding sites. One of the objectives of this work is to investigate the factors that affect the efficiency of potassium-ion transport across the membrane channel in the presence of disorder. The single particle system is described by a tight-binding Hamiltonian of the form

$$H\Big/\hbar = \sum_{j=1}^{6} \varepsilon_j \sigma_j^{\dagger}\sigma_j^{-} - c\sum_{j=2}^{4}\left(\sigma_j^{\dagger}\sigma_{j+1}^{-} + \sigma_{j+1}^{\dagger}\sigma_j^{-}\right), \tag{1}$$

where $\hbar$ is the reduced Planck constant, $c$ denotes the hopping rate between neighboring sites, and $j$ labels the lattice sites. The creation and annihilation operators at site $j$ are represented by $\sigma_j^{\dagger}$ and $\sigma_j^{-}$, respectively. In Equation 1, this tight-binding approach is commonly used to study quantum transport and tunneling phenomena, including those related to transport efficiency and quantum coherence in different ion channels (Vaziri and Plenio, 2010; Heinrichs, 1983).

The crucial element in this analysis is the set of on-site energies $\varepsilon_j$, where disorder is introduced by assigning correlated random values whose correlation strength is controlled by the parameter $A$, defined as (Buarque et al., 2023).

$$\tilde{\varepsilon}_j = \sum_m \frac{Z_m}{\left(1+\frac{d_{jm}}{A}\right)^2}, \tag{2}$$

where $Z_m \in [-1,1]$ are real numbers drawn from a uniform distribution, $d_{j,m} = |j-m|$ denotes the distance between sites $j$ and $m$, and $A$ sets the correlation length. Previous studies have shown that, in the unitary dynamics of large periodic lattices, increasing $A$ enhances the occurrence of high-amplitude wave intensities that are commonly referred to as rogue waves or extreme events, leading to a higher frequency of such events as the correlation strength grows (Buarque et al., 2023).

After generating each correlated sequence $\{\tilde{\varepsilon}_j\}$, the on-site energies are normalized to have zero mean and unit variance. This ensures that differences in transport properties arise from the correlation structure rather than from trivial changes in average energy or dispersion (da Silva and Prado, 2020). For a sequence of length $N$, we compute the average $\mu = \frac{1}{N}\sum_{j=1}^{N}\tilde{\varepsilon}_j$ and the variance $s^2 = \frac{1}{N}\sum_{j=1}^{N}(\tilde{\varepsilon}_j - \mu)^2$ in order to define the normalized energies as $\varepsilon_j = (\tilde{\varepsilon}_j - \mu)/s$.

The on-site energy sequences used in Equation 2 are intended to represent spatial fluctuations of the local site energies with a tunable degree of long-range correlation. The motivation for this choice is twofold. First, long-range correlations are known to alter interference patterns in wave systems and to produce rare, extreme amplitude events that strongly influence transport statistics in both classical and quantum settings. These extreme events correspond, in our discrete open chain, to configurations that transiently concentrate amplitude at certain sites, producing resonant trapping and markedly increasing traversal times. Second, spatial correlations of the kind modeled here can plausibly arise in biological ion channels: correlated positioning of charged or polar residues along the pore, collective conformational fluctuations of the protein scaffold, and correlated variations of the solvent/protein electrostatic environment (including lipid–protein coupling) can induce slowly varying, spatially correlated shifts of local site energies (Gu and de Groot, 2020; Chowdhury and Chanda, 2012; Goforth et al., 2003). Thus, Equation 2 represents a phenomenological, statistically controlled model for spatially correlated energetic landscapes whose transport consequences we explore in this paper.

Since the ion channel operates as an open quantum system, its dynamics are governed by the Lindblad master equation

$$\frac{d}{dt}\rho = -\frac{i}{\hbar}[H,\rho] + \mathcal{L}_s(\rho) + \mathcal{L}_d(\rho) + \mathcal{L}_{deph}(\rho), \tag{3}$$

where $\rho$ is the density matrix and $\mathcal{L}_{s/d}$ are Lindblad operators that model incoherent interactions with the environment given by

$$\mathcal{L}_s = \Gamma_s\left[2\sigma_2^{+}\sigma_1^{-}\rho\sigma_1^{+}\sigma_2^{-} - \{\sigma_1^{+}\sigma_2^{-}\sigma_2^{+}\sigma_1^{-},\rho\}\right] \tag{4}$$

and

$$\mathcal{L}_d = \Gamma_d\left[2\sigma_6^{+}\sigma_5^{-}\rho\sigma_5^{+}\sigma_6^{-} - \{\sigma_5^{+}\sigma_6^{-}\sigma_6^{+}\sigma_5^{-},\rho\}\right]. \tag{5}$$

where $\{\cdot,\cdot\}$ denotes the anticommutator operator.

In this framework, Equation 4, $\mathcal{L}_s$ represents the source (injection from the reservoir 1 into site 2), In Equation 5, $\mathcal{L}_d$ represents the drain (removal of population from site 5 to inject into site 6). The rates $\Gamma_s$ and $\Gamma_d$ determine the coupling strengths between the channel and its reservoirs. This formalism allows us to study the influence of correlated disorder on the transport efficiency by computing quantities such as the average time to reach the drain as a function of the correlation parameter $A$. It is also possible to simulate the effect of a random phase due to the system interaction with the environment modelled by:

$$\mathcal{L}_{\text{deph}}(\rho) = \sum_{j=2}^{5}\gamma_{\text{deph}}\left(-\{\sigma_j^{\dagger}\sigma_j,\rho\} + 2\sigma_j^{\dagger}\sigma_j\rho\sigma_j^{\dagger}\sigma_j\right), \tag{6}$$

where the dephasing rate is $\gamma_{deph}$. According to (De March et al., 2018; Contreras-Pulido et al., 2014; Moix et al., 2013), the dephasing produces an exponential decay of density matrix terms with rate $\gamma_{deph}$ which indicates quantum decoherence. In our simulations, the source and drain are modeled as components of the environment, functioning as classical reservoirs. The dephasing is applied to the four internal sites ($j = 2$ to $j = 5$) and is excluded from the source ($j = 1$) and the sink ($j = 6$) terms.

## 3 Results and discussion

All results presented in this work were obtained from an ensemble of 10,000 independent realizations of the disordered system. For each realization, the correlated on-site energies $\varepsilon_j$ were generated according to the prescribed correlation parameter $A$, and the Lindblad master equation was numerically integrated.

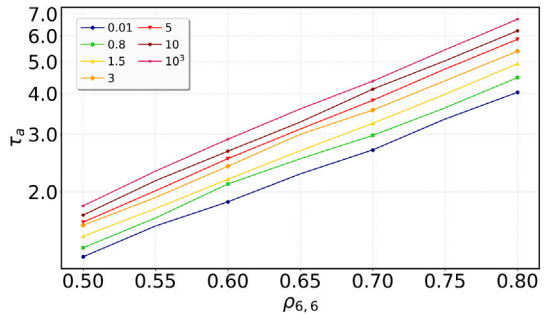


FIGURE 2
Average traversal time, $\tau_a$ (log scale), as a function of the drain occupation, $\rho_{6,6}$, obtained from 10,000 simulation runs. Results are shown for seven distinct values of the correlation parameter $A$, as indicated in the legend. The data reveal a clear logarithmic dependence of $\tau_a$ on $\rho_{6,6}$, as well as a systematic increase in the traversal time with increasing $A$.

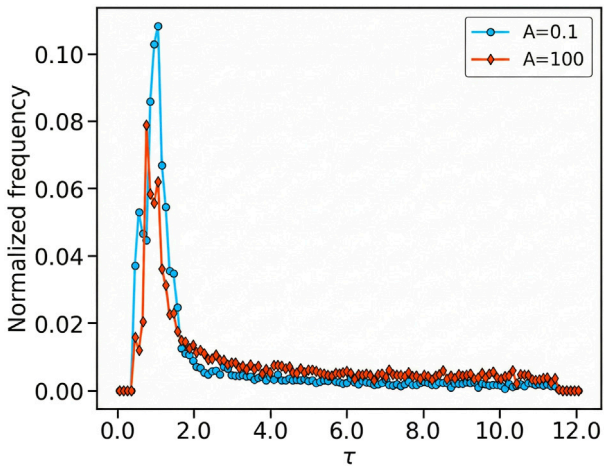


FIGURE 3
Traversal-time distributions obtained from an ensemble of 10,000 realizations, comparing weak ($A = 0.1$, blue circles) and strong ($A = 100$, orange diamonds) correlation regimes at a fixed drain occupation of $\rho_{6,6} \approx 0.65$. The strongly correlated case ($A = 100$) exhibits higher frequencies at longer traversal times. This feature reflects the presence of transient trapping events that induce significant delays in transport for a subset of realizations.

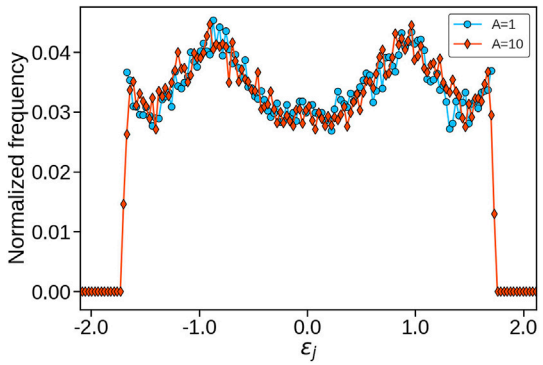


FIGURE 4
Distributions of on-site energies $\varepsilon_j$ for correlation parameters $A = 1$ (blue circles) and $A = 10$ (orange diamonds), computed over 10,000 realizations. The energies are normalized to ensure zero mean and unit variance, remaining bounded within the interval $[-2, 2]$.

For simplicity, we set $\hbar = 1$ and $c = 1$ in our simulations. When analysing our numerical results, the on-site energies as well as the source, drain, and dephasing rates are expressed in units of $c$. Powers of 10 are retained when making comparisons with values reported in the literature.

Ensemble averages were then computed over all realizations to obtain statistically representative quantities. We define $\tau$ as the traversal time, a dimensionless parameter defined as the physical time divided by $4\pi/c$, the characteristic time scale of the unitary dynamics (De March et al., 2018). Besides that, source and drain are set to have zero energy, and the initial state corresponds to the particle located at the source, $\rho_{1,1}$.

A physically grounded estimate for the hopping rate in quantum models of ion transport can be obtained from prior theoretical and computational studies of potassium channels. The effective site-to-site hopping rate in the selectivity filter was estimated to lie in the range $10^6 - 10^8 s^{-1}$, based on realistic coupling strengths and site-energy scales (Vaziri and Plenio, 2010). Subsequent extensions of this model including Coulomb interactions (De March et al., 2018), retained hopping rates in this same range while demonstrating that ion–ion repulsion constrains but does not suppress coherent transport. More recent quantum-biophysical analyses, including Lindblad-based treatments of coherence in ion channels (Seifi et al., 2022; Seifi et al., 2023), employ coupling parameters $c \sim 10^7 - 10^8 s^{-1}$ as appropriate for channels exhibiting high physiological flux. These values are also consistent with experimental conductance measurements of $K^+$ channels corresponding to $10^7 - 10^8$ ions per second, as well as with molecular-dynamics estimates in which individual transfer events occur on picosecond timescales, implying underlying microscopic transition rates up to $10^{11} - 10^{12} s^{-1}$. Together, these converging theoretical, computational, and experimental indications support using hopping and source/drain rates in the $10^6 - 10^8 s^{-1}$ range as physically plausible and biophysically well-motivated (De March et al., 2021).

As the traversal time $\tau$ is a key parameter in the study of ion channels, Figure 2 is presented to elucidate its behavior. The figure shows the average traversal time, $\tau_a$, computed from an ensemble of 10,000 realizations and plotted against the drain occupation ($\rho_{6,6}$) for seven values of the correlation parameter $A$, using a linear–log scale. Two main trends emerge from the data: a logarithmic dependence of $\tau_a$ on $\rho_{6,6}$ and a systematic increase in the traversal time with increasing $A$. The latter trend can be understood by examining the underlying traversal-time distribution, as shown in Figure 3.

As shown in Figure 3, the distribution undergoes a slight broadening while its peak position remains unchanged. For a drain occupation of 0.65, we see that while most realizations are concentrated at short times, a larger value of $A$ leads to more realizations with longer times. This indicates that the correlated disorder generates temporary trapping sites or resonant configurations that slow down transport by producing transient amplitude concentrations within the chain.

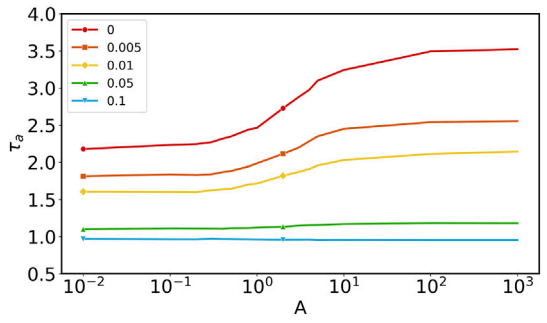


FIGURE 5
Mean traversal time $\tau_a$ as a function of the correlation parameter $A$ (log scale) for different dephasing rates $\gamma_{deph}$ values (in the legend). The drain occupation is fixed at $\rho_{6,6} = 0.65$. The plot illustrates the transition from a correlation-sensitive regime to a decoherence-dominated regime. At low dephasing rates (e.g., $\gamma_{deph} \leq 0.01$), the system retains quantum coherence, allowing correlated disorder to effectively trap the particle and increase $\tau_a$ logarithmically. Conversely, strong environmental coupling ($\gamma_{deph} > 0.01$) destroys phase information, suppressing the interference effects necessary for correlation-induced trapping, rendering the traversal time independent of $A$.

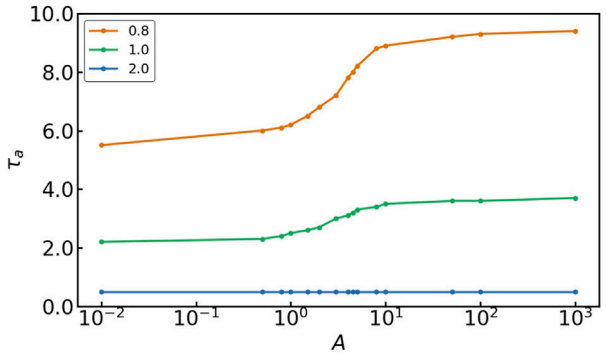


FIGURE 6
Mean traversal time, $\tau_a$, as a function of the correlation parameter $A$ (log scale) for three different hopping rates $c$. The drain occupation is fixed at $\rho_{6,6} = 0.65$. As $c$ becomes large compared to the on-site energy variance (unity), the average traversal time becomes essentially independent of $A$.

It is important to emphasize that the presence of transient trapping is not any trivial consequence of any broadening of the energy distribution generated by Equation 2, but rather a genuine effect of the correlations. To make this clear, Figure 4 shows the distributions of the on-site energies, $\varepsilon_j$, obtained from 10,000 realizations for two representative correlation strengths, $A = 1$ (weak correlation) and $A = 10$ (strong correlation). In both cases, the energies remain confined to the interval $[-2, 2]$ and exhibit only minor variations between the two regimes. The figure therefore mainly serves to highlight the fixed energy bounds, as the influence of the correlations is not directly reflected in this distribution.

The role of dephasing is expected to mitigate correlation effects, as biological environments are inherently noisy. Estimates for biomolecular systems indicate that realistic environmental dephasing rates in proteins at physiological temperature lie in the range $\gamma_{deph} \sim 10^{10} - 10^{12} s^{-1}$, consistent with quantum-transport models (Vaziri and Plenio, 2010; Seifi et al., 2023). Although very strong dephasing would suppress coherence-induced correlations, moderate dephasing can enhance transport, a phenomenon well documented in studies of disordered systems (Moix et al., 2013). For this reason, we focus on the weak-to-intermediate regime, $\gamma_{deph} = 0 - 0.1 \times 10^8 s^{-1}$, where coherence effects may still play a functional role.

The impact of random dephasing, implemented through the Lindblad operator in Equation 6, is shown in Figure 5. As indicated by the dephasing rates $\gamma_{deph}$ in the legend, the introduction of local phase noise progressively suppresses the system's sensitivity to on-site energy correlations. This trend is reflected in the convergence of the mean traversal times for different values of $A$ at large $\gamma_{\text{deph}}$. Importantly, the results also demonstrate that clear signatures of correlated disorder persist in the weak-dephasing regime.

Having addressed the environmental impact, we now consider the intrinsic transport scales. The interplay between the correlation parameter $A$ and the hopping rate $c$ is examined in Figure 6. When the hopping rate exceeds the variance of the on-site energies, the effect of correlations is strongly attenuated. Recall that the on-site energies lie within the range $[-2, 2]$, as shown in Figure 4, with zero mean and unit variance. Conversely, when the hopping amplitude is comparable to this variance, a clear dependence of the mean traversal time on $A$ emerges. This reinforces that correlated disorder most effectively delays transport when the hopping strength and the disorder variance are of similar magnitude. In summary, the ensemble simulations show that both the correlation strength and environmental factors (such as dephasing and hopping rate) play central roles in modulating transport dynamics described in Equation 3. These results provide a quantitative framework for understanding the balance between coherence and disorder in ion-channel–like quantum systems.

## 4 Conclusion

In this work, we investigated the impact of correlated disorder, environmental dephasing, and intrinsic transport parameters on quantum dynamics in a minimal model of the selectivity filter (SF) of ion channels. Using an open quantum system framework with a source, a drain, and four internal sites, we analyzed how correlations in the on-site energies influence the mean traversal time of particles crossing the channel.

Our numerical results show that increasing the correlation parameter $A$ leads to a logarithmic increase in the average traversal time $\tau_a$, reflecting a reduction in the frequency of rapid transmission events. This behavior is consistent with the formation of high-intensity wave patterns observed in larger correlated systems in previous studies, where strong correlations can generate temporary trapped states. Remarkably, our results reveal that a form of temporary trapping persists even in small open systems-despite the reduced system size and the presence of environmental coupling. This persistence is nontrivial and, indeed, surprising, as such trapping phenomena are generally associated with extended or closed systems rather than with minimal open channels.

Environmental dephasing, modeled through the Lindblad formalism, attenuates correlation-induced effects when the

dephasing rate is sufficiently large. However, signatures of correlated disorder remain visible under weak dephasing, consistent with estimated biomolecular dephasing rates reported in the literature for ion channels. Likewise, increasing the hopping rate, $c$, suppresses the sensitivity to correlations, indicating that strong tunneling diminishes the influence of energetic fluctuations. Correlation effects remain significant only when the hopping amplitude is comparable in magnitude to the variance of the on-site energies, which is also consistent with parameter regimes expected for realistic ion-channel models.

Taken together, these results demonstrate that transport efficiency in quantum models of biological ion channels arises from a subtle interplay between coherence and disorder. Correlated fluctuations can induce transient trapping even in small, open architectures, while moderate environmental noise and realistic hopping strengths allow transport to remain efficient. The parameter regimes explored here align with those proposed in the biophysical literature, reinforcing the physical relevance of the model and the robustness of the conclusions.

## Data availability statement

The raw data supporting the conclusions of this article will be made available by the authors, without undue reservation.

## Author contributions

ID: Conceptualization, Data curation, Formal Analysis, Investigation, Methodology, Software, Visualization, Writing – original draft, Writing – review and editing. RG: Conceptualization, Formal Analysis, Investigation, Methodology, Visualization, Writing – review and editing. LB: Conceptualization, Data curation, Formal Analysis, Investigation, Methodology, Project administration, Supervision, Validation, Visualization, Writing – original draft, Writing – review and editing. SP: Conceptualization, Data curation, Formal Analysis, Investigation, Methodology, Project administration, Software, Supervision, Validation, Visualization, Writing – original draft, Writing – review and editing.

## Funding

The author(s) declared that financial support was received for this work and/or its publication. The authors declare that this research was conducted during the tenure of a scholarship from CNPq (Brazil). No specific funding from CNPq was received for the publication fees of this article.

## Acknowledgements

IPSR acknowledges the financial support provided by CNPq. IPSR and RGL also express their gratitude to the Ciência Pioneira initiative for organizing the Quantum Biology School, which was instrumental to this work, and especially thank Dr. Clarice Aiello, Dr. Marcelo Sousa, and the entire Ciência Pioneira team.

## Conflict of interest

The author(s) declared that this work was conducted in the absence of any commercial or financial relationships that could be construed as a potential conflict of interest.

## Generative AI statement

The author(s) declared that generative AI was not used in the creation of this manuscript.

Any alternative text (alt text) provided alongside figures in this article has been generated by Frontiers with the support of artificial intelligence and reasonable efforts have been made to ensure accuracy, including review by the authors wherever possible. If you identify any issues, please contact us.

## Publisher's note

All claims expressed in this article are solely those of the authors and do not necessarily represent those of their affiliated organizations, or those of the publisher, the editors and the reviewers. Any product that may be evaluated in this article, or claim that may be made by its manufacturer, is not guaranteed or endorsed by the publisher.

## Supplementary material

The Supplementary Material for this article can be found online at: https://www.frontiersin.org/articles/10.3389/frqst.2025.1725290/full#supplementary-material

## References

Aiello, C. D., Abendroth, J. M., Abbas, M., Afanasev, A., Agarwal, S., Banerjee, A. S., et al. (2022). A chirality-based quantum leap. *ACS Nano* 16, 4989–5035. doi:10.1021/acsnano.1c01347

Almeida, G. M., de Moura, F. A., and Lyra, M. L. (2018). Quantum-state transfer through long-range correlated disordered channels. *Phys. Lett. A* 382, 1335–1340. doi:10.1016/j.physleta.2018.03.028

Alvarez, P. H., Chowdhury, F. T., Smith, L. D., Brokowski, T. J., Aiello, C. D., Kattnig, D. R., et al. (2024). Simulating spin biology using a digital quantum computer: prospects on a near-term quantum hardware emulator. *Apl. Quantum* 1, 036114. doi:10.1063/5.0213120

Berneche, S., and Roux, B. (2001). Energetics of ion conduction through the K+ channel. *Nature* 414, 73–77. doi:10.1038/35102067

Bonatto, C., Prado, S. D., Metz, F. L., Schoffen, J. R., Correia, R. R. B., and Hickmann, J. M. (2020). Super rogue wave generation in the linear regime. *Phys. Rev. E* 102, 052219. doi:10.1103/PhysRevE.102.052219

Brookes, J. C. (2017). Quantum effects in biology: golden rule in enzymes, olfaction, photosynthesis and magnetodetection. *Proc. R. Soc. A Math. Phys. Eng. Sci.* 473, 20160822. doi:10.1098/rspa.2016.0822

Buarque, A., Dias, W., Almeida, G., Lyra, M., and de Moura, F. (2023). Rogue waves in quantum lattices with correlated disorder. *Phys. Rev. A* 107, 012425. doi:10.1103/physreva.107.012425

Chowdhury, S., and Chanda, B. (2012). Thermodynamics of electromechanical coupling in voltage-gated ion channels. *J. General Physiology* 140, 613–628. doi:10.1085/jgp.201210840

Collini, E., Wong, C. Y., Wilk, K. E., Curmi, P. M., Brumer, P., and Scholes, G. D. (2010). Coherently wired light-harvesting in photosynthetic marine algae at ambient temperature. *Nature* 463, 644–647. doi:10.1038/nature08811

Contreras-Pulido, L., Bruderer, M., Huelga, S. F., and Plenio, M. B. (2014). Dephasing-assisted transport in linear triple quantum dots. *New J. Phys.* 16, 113061. doi:10.1088/1367-2630/16/11/113061

De March, N., Prado, S. D., and Brunnet, L. G. (2018). Coulomb interaction rules timescales in potassium ion channel tunneling. *J. Phys. Condens. Matter* 30, 255101. doi:10.1088/1361-648X/aac40b

da Silva, R., and Prado, S. D. (2020). A simple study of the correlation effects in the superposition of waves of electric fields: the emergence of extreme events. *Phys. Lett. A* 384, 162231. doi:10.1016/j.physleta.2019.126231

De March, N., Prado, S. D., and Brunnet, L. G. (2021). Transport threshold in a quantum model for the ksca ion channel. *J. Phys. Condens. Matter* 34, 025101. doi:10.1088/1361-648x/ac2cf0

Doyle, D. A., Cabral, J. M., Pfuetzner, R. A., Kuo, A., Gulbis, J. M., Cohen, S. L., et al. (1998). The structure of the potassium channel: molecular basis of k+ conduction and selectivity. *Science* 280, 69–77. doi:10.1126/science.280.5360.69

Engel, G. S., Calhoun, T. R., Read, E. L., Ahn, T.-K., Mančal, T., Cheng, Y.-C., et al. (2007). Evidence for wavelike energy transfer through quantum coherence in photosynthetic systems. *Nature* 446, 782–786. doi:10.1038/nature05678

Goforth, R. L., Chi, A. K., Greathouse, D. V., Providence, L. L., Koeppe II, R. E., and Andersen, O. S. (2003). Hydrophobic coupling of lipid bilayer energetics to channel function. *J. General Physiology* 121, 477–493. doi:10.1085/jgp.200308797

Gu, R.-X., and de Groot, B. L. (2020). Lipid–protein interactions modulate the conformational equilibrium of a potassium channel. *Nat. Commun.* 11, 1–10. doi:10.1038/s41467-020-15741-8

Gwan, J.-F., and Baumgaertner, A. (2007). Cooperative transport in a potassium ion channel. *J. Chemical Physics* 127, 045103. doi:10.1063/1.2756531

Heinrichs, J. (1983). Quantum transport in dynamically disordered continuum tight binding systems. *Z. für Phys. B Condens. Matter* 52, 9–18. doi:10.1007/bf01305893

Hore, P. J., and Mouritsen, H. (2016). The radical-pair mechanism of magnetoreception. *Annu. Review Biophysics* 45, 299–344. doi:10.1146/annurev-biophys-032116-094545

Izrailev, F. M., Krokhin, A. A., and Makarov, N. (2012). Anomalous localization in low-dimensional systems with correlated disorder. *Phys. Rep.* 512, 125–254. doi:10.1016/j.physrep.2011.11.002

Jalalinejad, A., Bassereh, H., Salari, V., Ala-Nissila, T., and Giacometti, A. (2018). Excitation energy transport with noise and disorder in a model of the selectivity filter of an ion channel. *J. Phys. Condens. Matter* 30, 415101. doi:10.1088/1361-648X/aadeab

McFadden, J., and Al-Khalili, J. (1999). A quantum mechanical model of adaptive mutation. *Biosystems* 50, 203–211. doi:10.1016/s0303-2647(99)00004-0

Mohseni, M., Rebentrost, P., Lloyd, S., and Aspuru-Guzik, A. (2008). Environment-assisted quantum walks in energy transfer of photosynthetic complexes. *J. Chem. Phys.* 129, 174106. doi:10.1063/1.3002335

Moix, J. M., Khasin, M., and Cao, J. (2013). Coherent quantum transport in disordered systems: I. the influence of dephasing on the transport properties and absorption spectra on one-dimensional systems. *New J. Phys.* 15, 085010. doi:10.1088/1367-2630/15/8/085010

Plenio, M. B., and Huelga, S. F. (2008). Dephasing-assisted transport: quantum networks and biomolecules. *New J. Phys.* 10, 113019. doi:10.1088/1367-2630/10/11/113019

Polakowski, M., and Panfil, M. (2024). Quantum features of the transport through ion channels in the soft knock-on model. *Phys. Biol.* 22, 016007. doi:10.1088/1478-3975/ad9cde

Salari, V., Naeij, H., and Shafiee, A. (2017). Quantum interference and selectivity through biological ion channels. *Sci. Reports* 7, 41625. doi:10.1038/srep41625

Sarovar, M., Ishizaki, A., Fleming, G. R., and Whaley, K. B. (2010). Quantum entanglement in photosynthetic light-harvesting complexes. *Nat. Phys.* 6, 462–467. doi:10.1038/nphys1652

Seifi, B., Soltanmanesh, A., and Shafiee, M. (2022). Quantum coherence on selectivity and transport of ion channels. *Sci. Rep.* 12, 9300. doi:10.1038/s41598-022-13323-w

Seifi, B., Soltanmanesh, A., and Shafiee, M. (2023). Mimicking classical noise in ion channels by quantum decoherence. *J. Biol. Phys.* 49, 295–317.

Vaziri, A., and Plenio, M. B. (2010). Quantum coherence in ion channels: resonances, transport and verification. *New J. Phys.* 12, 085001. doi:10.1088/1367-2630/12/8/085001